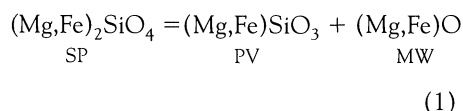


The Effect of Alumina on Phase Transformations at the 660-Kilometer Discontinuity from Fe-Mg Partitioning Experiments

B. J. Wood and D. C. Rubie

Experimental data on the partitioning of Fe and Mg between coexisting silicate perovskite, magnesiowüstite, and γ -(Mg,Fe)₂SiO₄ demonstrate that Fe substitution in perovskite is strongly coupled to Al₂O₃ concentration. In Al₂O₃-free compositions, perovskite has a low Fe/(Fe+Mg) ratio: for a bulk Fe/(Fe+Mg) of 0.11, perovskite has a value close to 0.04, whereas magnesiowüstite has a ratio near 0.17. In peridotitic mantle, however, where the perovskite should contain 4 to 5 weight percent Al₂O₃, it has essentially the same Fe/(Fe+Mg) ratio as coexisting magnesiowüstite. Under lower mantle conditions, therefore, perovskite and magnesiowüstite should, in peridotite, each have an Fe/(Fe+Mg) ratio close to 0.11.

The seismic discontinuity at 660-km depth is a global feature, dividing Earth's lower mantle from the overlying transition zone and upper mantle. It corresponds to 6 to 10% increases in seismic wave velocity and density with increasing depth (1). Recent experiments (2-4) have demonstrated that the 660-km discontinuity corresponds in pressure (23.5 GPa) and temperature (approximately 1600°C) to the conditions of the decomposition of γ -(Mg,Fe)₂SiO₄ spinel (SP), the major constituent of peridotite at this depth (3), into (Mg,Fe)SiO₃ perovskite (PV) and (Mg,Fe)O magnesiowüstite (MW)



The documentation of such conditions means that a qualitative interpretation of the 660-km discontinuity can be provided by the occurrence of reaction 1 in an approximately peridotitic mantle (3). Better constraints on average mantle composition are, in principle, provided by the sharpness and magnitudes of density and seismic velocity changes at the 660-km discontinuity and from velocity and density gradients in the lower mantle (5). However, in order to compare seismically determined density and velocity structure with laboratory-measured

elastic properties and densities of minerals, it is necessary to know how the chemical components of the mantle distribute themselves between the different minerals present. Currently, the partitioning of FeO, MgO, and other major components such as Al₂O₃ between perovskite and magnesiowüstite is poorly constrained for peridotitic and other natural compositions. Therefore, partitioning behavior must be assumed, yielding uncertain estimates of bulk rock properties. The partitioning assumptions are important because density and elastic properties depend substantially on compositional parameters such as Fe#, the molar ratio Fe/(Fe+Mg). Here we determine the partitioning of Fe and Mg between spinel, perovskite, and magnesiowüstite in bulk compositions that reflect natural abundanc-

es of minor components such as Al₂O₃ in order to obtain better estimates of mineral compositions under lower mantle conditions. The results are also applied to an understanding of the reactions at depths between 660 and 750 km.

All experiments were performed on the multianvil apparatus at the Bayerisches Geoinstitut, and analyses were made with the JEOL 8600 microprobe at the University of Bristol (6). Our data (Table 1) on the partitioning of Fe and Mg between spinel and magnesiowüstite in compositions doped with about 1% each of Al₂O₃, MnO, Cr₂O₃, and NiO are consistent with previous results (4, 7, 8) in both peridotitic bulk compositions and in the simple system MgO-FeO-SiO₂. The magnesiowüstite is always substantially richer in Fe than is coexisting spinel. For typical peridotite with an Fe# in spinel of 0.11, the coexisting magnesiowüstite would have an Fe# of 0.166. On the basis of a comparison with previous results, we find that doping with Al₂O₃, MnO, Cr₂O₃, and NiO does not significantly affect the Fe-Mg partitioning between spinel and magnesiowüstite. Partitioning data for Fe and Mg between perovskite and magnesiowüstite in Al₂O₃-free compositions (8-11) indicate that perovskite in equilibrium with magnesiowüstite contains very little Fe. A perovskite Fe# of about 0.04 would be appropriate for equilibrium, with magnesiowüstite and spinel having Fe# of 0.166 and 0.11, respectively (that is, for peridotite mantle composition) (8-11). In contrast to spinel-magnesiowüstite relations, which are insensitive to the presence of other components, this result can only apply in the absence of Al₂O₃.

Fertile peridotites such as "pyrolite" (12) contain 3.0 to 4.0 weight % Al₂O₃, most of which should, in the lower mantle, reside in the Mg-rich perovskite phase, with lesser amounts in magnesiowüstite and Ca perovskite (2, 7). In a peridotitic composition, the perovskite phase constitutes about 75% of

Table 1. Experimental data: pressure (*P*), temperature (*T*), and compositions. Experiments at 25 GPa in Mo capsules exhibited Fe loss to the capsule and precipitation of Mo-Fe alloy in the charge. Runs in Re capsules contained excess ReO₂ to maintain oxidizing conditions. MW, magnesiowüstite; OL, olivine; SP, spinel; OP, orthopyroxene; and PV, perovskite. Numbers in parentheses refer to Fe# and weight % Al₂O₃.

<i>P</i> (GPa)	<i>T</i> (°C)	Starting composition	Capsule	Final composition
20.4	1600	MW(0.28,0.5), OL(0.104,0.0)	Mo	MW(0.25,0.5), SP(0.16,0.4)
20.4	1600	MW(0.46,0.4), OL(0.104,0.0)	Mo	MW(0.36,0.3), SP(0.22,0.2)
25	1600	MW(0.17,5.0), OP(0.10,0.0)	Re	MW(0.125,0.1), PV(0.155,6.8)
25	1600	MW(0.17,5.0), OP(0.21,4.1)	Re	MW(0.168,0.1), PV(0.195,8.9)
25	1500	MW(0.17,5.0), OP(0.21,4.1)	Fe	MW(0.185,1.5), PV(0.185,4.3)*
25	1600	MW(0.46,0.4), OP(0.21,4.1)	Mo	MW(0.154,0.7), PV(0.180,4.0)
25	1600	MW(0.28,0.5), OP(0.10,3.6)	Mo	MW(0.094,0.3), PV(0.096,4.1)
25	1600	MW(0.17,5.0), OP(0.21,4.1)	Mo	MW(0.121,1.3), PV(0.169,4.5)*
25	1600	MW(0.17,5.0), OP(0.21,4.1)	Mo	MW(0.151,2.3), PV(0.188,5.0)

*A small amount of an unidentified aluminous phase was present.

B. J. Wood, Department of Geology, University of Bristol, Bristol BS8 1 RJ, UK.
D. C. Rubie, Bayerisches Geoinstitut, Universität Bayreuth, D-95440 Bayreuth, Germany.

the rock by weight, which gives it an Al_2O_3 concentration, under lower mantle conditions, of 4.0 to 5.3 weight %. In our study, experiments on mixtures of orthopyroxene (0.0 to 4.1 weight % Al_2O_3) and magnesiowüstite (0.4 to 5.0 weight % Al_2O_3) produced perovskite-magnesiowüstite assemblages in which the perovskite and magnesiowüstite contained 4.0 to 8.9 and 0.1 to 2.3 weight % Al_2O_3 , respectively (6). The results (Fig. 1) demonstrate a substantial shift in Fe-Mg partitioning between perovskite and magnesiowüstite in alumina-bearing bulk compositions relative to Al_2O_3 -free compositions. Our measurements (6) [consistent with those from (7, 13)] indicate that in the presence of Al_2O_3 , the two phases have approximately equal values of Fe#. When applying our results to the Earth, some uncertainty arises from the unknown oxidation state of Fe in the products. However, experiments performed in both reducing (Fe capsule) and oxidizing (Re capsule + excess ReO_2) environments showed similar large partitioning shifts relative to the Al_2O_3 -free system (6) (Fig. 1), indicating that our results should apply under any conceivable lower mantle conditions.

At a depth slightly shallower than 660 km, peridotitic mantle (plotted on Fig. 2) consists of 60 to 70% spinel, 30% garnet containing 12 weight % Al_2O_3 , and small amounts of a calcium silicate perovskite (2, 3). Two possible reaction models arise depending on whether or not $(Mg,Fe)SiO_3$ perovskite can contain 4 to 5 weight % Al_2O_3 when it first appears at 660-km depth. If the first perovskite to appear is low in Al_2O_3 , then tie lines **a**, **b**, **c**, and **f** in Fig. 2 are applicable at 660 km. In this case, be-

cause perovskite, spinel, and magnesiowüstite compositions are collinear on Fig. 2, reaction 1 is pseudounivariant, taking place over a very narrow depth interval (14). Immediately below 660 km, therefore, spinel would completely disappear, and the mantle would consist of about 30% each of perovskite, magnesiowüstite, and garnet, with 10% minor phases (Fig. 3). Our experiments [also see (2, 3, 7)] demonstrate, however, that perovskite can contain up to 8.9 weight % Al_2O_3 at about 25 GPa, which means that aluminous garnet must dissolve into perovskite with increasing depth and eventually disappear from peridotite compositions at 700 to 750 km. The likely consequences are shown in Fig. 3. As the Al_2O_3 -content of perovskite increases, the perovskite must, from the measured partitioning relations, become more Fe-rich. At the same time, because the bulk peridotite composition has fixed Fe#, the magnesiowüstite and residual garnet must become poorer in Fe to compensate. The net effect is a rotation of the **a** and **b** tie lines (Fig. 3). Garnet will completely disappear at about the point where the **ab** tie line cuts the peridotite bulk composition. The mantle below 750 km will then have the compositional relations shown by the dotted line in Fig. 3. This model leads to a sharp 660-km discontinuity caused by spinel breakdown, followed by abnormal gradients in density and velocity to about 750 km as garnet dissolves into perovskite and the **ab** tie line rotates.

The second possibility is that Al_2O_3 -rich perovskite is stable when it first appears,

which would mean that tie lines **b**, **c**, **d**, and **e** (Fig. 2) are appropriate at 660 km. In this case, because mantle peridotite has a low Fe# of 0.11, only small amounts of Fe-rich perovskite and magnesiowüstite can be produced at 660 km. However, these phases become progressively more stable than spinel and garnet below 660 km, so they must increase in amount with increasing depth. As perovskite and magnesiowüstite increase in amount, all four minerals must move to lower Fe# to preserve the relative partitioning relations at the fixed peridotite bulk composition. With increasing depth, therefore, mineral compositions and tie lines **b**, **c**, **d**, and **e** will all move to lower Fe# as spinel and garnet are consumed and perovskite and magnesiowüstite are produced. This process continues until tie line **e** crosses the mantle composition, at which point, as before, all of the spinel and garnet are gone. In this case, the 660-km discontinuity would not be sharp because spinel and garnet would disappear gradually over a considerable depth interval. There would, however, be steep gradients in velocity and density within the reaction interval (approximately 660 to 750 km) as perovskite and magnesiowüstite are produced. Below 750 km, the perovskite and magnesiowüstite compositions would be the same as those shown by the dotted line in Fig. 3, which reflects partitioning for Al_2O_3 -rich perovskite.

Because of pressure uncertainties in the multianvil apparatus [about 5 to 10% (13, 15)], it is currently almost impossible to test experimentally which model actually applies to the interval between 660 and 750 km. Seismological data, however, strongly support the tie-line rotation model of Fig. 3. Recent seismic studies using large arrays (16) and stacking techniques (17) demonstrated that the 660-km discontinuity is a

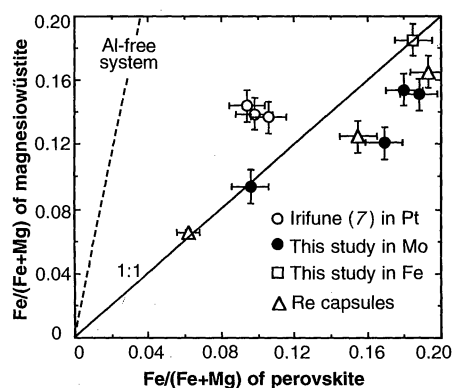


Fig. 1. Partitioning of Fe-Mg between (Mg,Fe,Al) perovskite and magnesiowüstite. Note the dramatic shift relative to the Al_2O_3 -free system caused by the addition of Al_2O_3 (4.0 to 8.9 weight %) to perovskite. The oxidation state imposed by the capsule from Fe (reducing) to Re (relatively oxidizing) appears to have little effect. The two points in Re capsules at high Fe# are from this study, and that at low Fe# is from (13) at the higher temperature of $2400^\circ \pm 100^\circ C$.

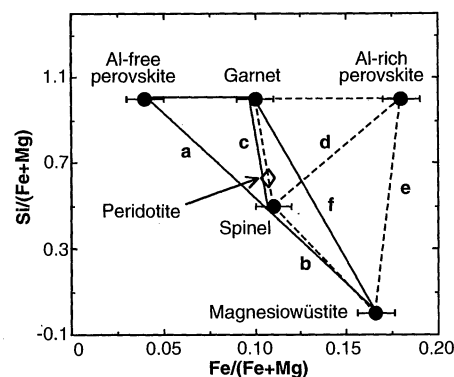


Fig. 2. Observed Fe-Mg partitioning between perovskite, magnesiowüstite, garnet, and spinel under conditions approximating those of the 660-km discontinuity. Two perovskite points are plotted, reflecting Fe# for Al_2O_3 -free and Al_2O_3 -rich (approximately 5 weight %) compositions in equilibrium with spinel of Fe# = 0.11. The results lead to two possible models of the reactions in peridotite between depths of 660 and about 750 km. Illustrative tie-lines **a**, **b**, **c**, and **f** link equilibrium compositions together if perovskite is essentially Al_2O_3 -free when it first appears; dashed tie-lines **b**, **c**, **d**, and **e** apply if perovskite is Al_2O_3 -rich (approximately 5 weight %) when it appears.

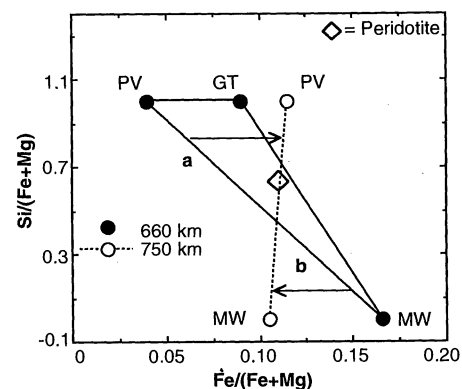


Fig. 3. Changing phase relations between depths of 660 and 750 km under the assumption that Al_2O_3 -poor perovskite (PV) and magnesiowüstite (MW) first appear at 660 km by pseudounivariant breakdown of spinel. With increasing depth, the aluminous garnet (GT) dissolves into perovskite, and the perovskite-magnesiowüstite tie-lines **a** and **b** rotate as shown.

relatively strong reflector in the 0.2- to 0.5-Hz range, requiring that substantial changes in elastic properties take place over a narrow 5- to 12-km depth interval (16, 17). This constraint means that the major reaction, spinel breakdown, must be pseudounivariant, which is only consistent with perovskite being Al_2O_3 -poor at the 660-km discontinuity. In addition, global seismological models (1) indicate that the region between 660 and 750 km exhibits steeper velocity-depth gradients than the region below 750 km, which would be consistent with the gradual dissolution of garnet into perovskite accompanied by tie-line rotation. Whichever model is correct, perovskite and magnesio-wüstite in peridotite must have similar values of Fe# (0.11) under lower mantle conditions, a fact that impacts physical properties of the mantle such as density and electrical conductivity.

From the standpoint of crystal chemistry, it is interesting and unusual that Al_2O_3 has such a large effect on the Fe content of perovskite. Kesson *et al.* (18) observed that perovskites with up to 25 weight % Al_2O_3 could be synthesized at 60 GPa on the join $\text{Mg}_3\text{Al}_2\text{Si}_3\text{O}_{12}$ - $\text{Fe}_3\text{Al}_2\text{Si}_3\text{O}_{12}$ for all values of Fe# between 0.0 and 0.75. Perovskites much richer in Fe and Al than those of this study are therefore stable under deeper mantle conditions. Coupling between Al and Fe may be inferred from comparison with the work of Ito and Takahashi (19), who found only 1.3 weight % Al_2O_3 in pure MgSiO_3 perovskite, in contrast to 8.9 weight % in $(\text{Mg,Fe})\text{SiO}_3$ found by us under the same pressure-temperature conditions. Although the Fe oxidation state in product perovskites is unknown, one possible explanation for the apparent Fe-Al coupling is that a substantial part of the Fe enters as Fe^{3+} through solution of the component $\text{Fe}^{\text{III}}\text{AlO}_3$. This hypothetical perovskite would have Fe^{3+} on the dodecahedral site and Al^{3+} on the octahedral site. The presence of this component seems more likely than the alternative, that small amounts of octahedral Al^{3+} dramatically change the thermodynamic properties of Fe^{2+} on the dodecahedral site.

REFERENCES AND NOTES

1. A. M. Dziewonski and D. L. Anderson, *Phys. Earth Planet. Inter.* **25**, 297 (1981); B. L. N. Kennett, E. R. Engdahl, R. Buland, *Geophys. J. Int.* **122**, 108 (1995).
2. T. Irifune and A. E. Ringwood, *Geophys. Monogr. Am. Geophys. Union* **39**, 231 (1987).
3. A. E. Ringwood, *Geochim. Cosmochim. Acta* **55**, 2083 (1991).
4. E. Ito and E. Takahashi, *J. Geophys. Res.* **94**, 10637 (1989).
5. L. Stixrude, R. J. Hemley, Y. Fei, H. K. Mao, *Science* **257**, 1099 (1992); E. Knittle, R. Jeanloz, G. L. Smith, *Nature* **319**, 214 (1986); J. Ita and L. Stixrude, *J. Geophys. Res.* **97**, 6849 (1992).

6. Starting materials for experiments were mainly ground mixtures of natural minerals from peridotite xenoliths and synthetic magnesio-wüstites. Magnesio-wüstites ($\text{Mg}_{1-x}\text{Fe}_x\text{O}$ ($x = 0.28$ and 0.46)) were doped with up to 1 weight % each of Al_2O_3 , Cr_2O_3 , NiO , and MnO . Magnesio-wüstite of $x = 0.17$ contained about 5 weight % Al_2O_3 and no other dopant. Natural orthopyroxenes contained 3.6 to 4.1 weight % Al_2O_3 and 0.5 weight % CaO in addition to having Fe# values of 0.10 and 0.21. A partially reacted oxide mix of composition $(\text{Mg}_{0.9}\text{Fe}_{0.1})\text{SiO}_3$ without Al_2O_3 was used in one experiment. Natural olivine had the composition $(\text{Mg}_{0.896}\text{Fe}_{0.104})_2\text{SiO}_4$. All starting materials were examined by ^{57}Fe Mössbauer spectroscopy and were found to have an $\text{Fe}^{3+}/\text{Fe}^{2+}$ ratio of 0.05 or less. Samples were encapsulated in Mo, Re, or Fe capsules and heated at 1600°C (appropriate for 660-km depth [J. M. Brown and T. J. Shankland, *Geophys. J. R. Astron. Soc.* **66**, 579 (1981)]) or 1500°C for 3 hours after pressurization to either 20.4 GPa (for spinel-bearing assemblages) or 25 GPa (for perovskite). Multianvil assemblies and pressure calibrations have been described previously (13, 15). The products were examined by x-ray diffraction, and compositions were determined with the JEOL 8600 electron microprobe at the University of Bristol. All compositions were determined by averaging 10 or more individual point analyses. Experimental data given in Table 1.
7. T. Irifune, *Nature* **370**, 131 (1994).
8. Y. Fei, H.-K. Mao, B. O. Mysen, *J. Geophys. Res.* **96**, 2157 (1991).
9. One datum obtained in this study was from a natural $(\text{Mg}_{0.896}\text{Fe}_{0.104})_2\text{SiO}_4$ olivine, which, at 25 GPa and

1600°C, decomposed into a fine intergrowth of perovskite and magnesio-wüstite. Because individual crystals were not resolvable with the electron microprobe, the variation of Fe# with Si content was used to extrapolate to end-member compositions in the same manner as that used by Guyot *et al.* (10) and Fei *et al.* (8). We obtained an Fe# of 0.04 ± 0.02 for perovskite and 0.15 ± 0.02 for magnesio-wüstite.

10. F. Guyot, M. Madon, J. Peyronneau, J. P. Poirier, *Earth Planet. Sci. Lett.* **90**, 52 (1988).
11. E. Ito, E. Takahashi, Y. Matsui, *ibid.* **67**, 238 (1984).
12. A. E. Ringwood, *Composition and Petrology of the Earth's Mantle* (McGraw-Hill, New York, 1975).
13. E. A. McFarlane, M. J. Drake, D. C. Rubie, *Geochim. Cosmochim. Acta* **58**, 5161 (1994).
14. B. J. Wood, *J. Geophys. Res.* **95**, 12681 (1990).
15. D. Canil, *Phys. Earth Planet. Inter.* **86**, 25 (1994).
16. H. M. Benz and J. E. Vidale, *Nature* **365**, 147 (1993); A. Yamazaki and K. Hirahara, *Geophys. Res. Lett.* **21**, 1811 (1994).
17. H. Paulssen, *J. Geophys. Res.* **93**, 10489 (1988).
18. S. E. Kesson, J. D. Fitzgerald, J. M. G. Shelley, R. L. Withers, *Earth Planet. Sci. Lett.* **134**, 187 (1995).
19. E. Ito and E. Takahashi, *Geophys. Monogr. Am. Geophys. Union* **39**, 21 (1987).
20. Multianvil experiments were performed at the Bayerisches Geoinstitut under the European Community "Human Capital and Mobility—Access to Large Scale Facilities" programme (contract ERBCH-GECT940053 to D.C.R.). B.J.W. acknowledges the support of the Alexander von Humboldt Stiftung during preparation of the manuscript.

13 May 1996; accepted 17 July 1996

Iridium in Natural Waters

A. D. Anbar,* G. J. Wasserburg, D. A. Papanastassiou, P. S. Andersson

Iridium, commonly used as a tracer of extraterrestrial material, was measured in rivers, oceans, and an estuarine environment. The concentration of iridium in the oceans ranges from $3.0 (\pm 1.3) \times 10^8$ to $5.7 (\pm 0.8) \times 10^8$ atoms per kilogram. Rivers contain from $17.4 (\pm 0.9) \times 10^8$ to $92.9 (\pm 2.2) \times 10^8$ atoms per kilogram and supply more dissolved iridium to the oceans than do extraterrestrial sources. In the Baltic Sea, ~75% of riverine iridium is removed from solution. Iron-manganese oxyhydroxides scavenge iridium under oxidizing conditions, but anoxic environments are not a major sink for iridium. The ocean residence time of iridium is between 2×10^3 and 2×10^4 years.

Iridium and the other platinum group elements (PGEs) are used as tracers of extraterrestrial material because these elements are enriched in meteorites relative to Earth's crust (1). The high concentration of Ir in sediments and rocks at the Cretaceous-Tertiary (K-T) boundary is thought to be the result of an extraterrestrial impact that caused mass extinction (2). Smaller Ir en-

richments are coincident with other extinction horizons (3). The long-term extraterrestrial flux is quantified from the Ir burial flux recorded in deep-sea sediments (4). Understanding the aqueous geochemistry of Ir is important because most sediments are deposited in aquatic environments and may be subject to aqueous alteration after deposition. Low concentrations of Ir in natural waters have limited the study of its geochemistry. However, recent advances in negative thermal ionization mass spectrometry (NTIMS) provide the sensitivity to measure Ir in typical crustal materials (5). In combination with ultraclean chemical separation techniques, we used isotope dilution and NTIMS to characterize the natural water chemistry of Ir. This method permits the analysis of Ir in as little as 4 liters of water from the open ocean (6, 7), a

A. D. Anbar, G. J. Wasserburg, D. A. Papanastassiou, The Lунatic Asylum of the Charles Arms Laboratory, Division of Geological and Planetary Sciences, California Institute of Technology, Pasadena, CA 91125, USA.
P. S. Andersson, Laboratory for Isotope Geology, Swedish Museum of Natural History, S-104 05 Stockholm, Sweden.

*To whom correspondence should be addressed. Present address: Department of Earth and Environmental Sciences and Department of Chemistry, University of Rochester, Rochester, NY 14627, USA. E-mail: anbar@earth.rochester.edu